Pressure effects on the superconducting transition in *nH*-CaAlSi

L. Boeri,[1] J. S. Kim,[1] M. Giantomassi,[2] F. S. Razavi,[3] S. Kuroiwa,[4] J. Akimitsu,[4] and R. K. Kremer[1]
[1]*Max-Planck-Institut für Festkörperforschung, Heisenbergstraße 1, 70569 Stuttgart, Germany*
[2]*Unité de Physico-Chimie et de Physique des Matériaux, Université Catholique de Louvain, 1 Place Croix du Sud, B-1348 Louvain-la-Neuve, Belgium*
[3]*Department of Physics, Brock University, St. Catharines, Ontario, Canada L2S 3A1*
[4]*Department of Physics and Mathematics, Aoyama-Gakuin University, Sagamihara, Kanagawa 229-8558, Japan*
(Received 13 December 2007; revised manuscript received 14 February 2008; published 1 April 2008)

We present a combined experimental and theoretical study of the effects of pressure on T_c of the hexagonal layered superconductors *nH*-CaAlSi ($n=1$, 5, and 6), where *nH* denotes the different stacking variants that were recently discovered. Experimentally, the pressure dependence of T_c has been investigated by measuring the magnetic susceptibility of single crystals up to 10 kbars. In contrast to previous results on polycrystalline samples, single crystals with different stacking sequences display different pressure dependences of T_c. 1*H*-CaAlSi shows a decrease in T_c with pressure, whereas 5*H*- and 6*H*-CaAlSi exhibit an increase in T_c with pressure. *Ab initio* calculations for 1*H*-, 5*H*-, and 6*H*-CaAlSi reveal that an ultrasoft phonon branch associated with out-of-plane vibrations of the Al-Si layers softens with pressure, leading to a structural instability at high pressures. For 1*H*-CaAlSi, the softening is not sufficient to cause an increase in T_c, which is consistent with the present experiments but adverse to previous reports. For 5*H* and 6*H*, the softening provides the mechanism to understand the observed increase in T_c with pressure. Calculations for hypothetical 2*H* and 3*H* stacking variants reveal qualitative and quantitative differences.

DOI: 10.1103/PhysRevB.77.144502 PACS number(s): 74.70.Dd, 74.62.Fj, 74.25.Kc

Superconductivity in hexagonal layered compounds has attracted a lot of interest since the discovery of "high-T_c" superconductivity in MgB_2 (Ref. 1) and other structurally related compounds such as (Ca,Sr)AlSi,[2] $CaSi_2$,[3] and, very recently, alkaline-earth intercalated graphites.[4–6] In all of these compounds, the light elements are arranged in honeycomb layers that are intercalated by alkaline-earth atoms. Depending on the elements forming the honeycomb layer, the electron and phonon states involved in the superconducting pairing are quite different. In MgB_2, the holes in the σ bands of the *B* layer strongly couple to *B* bond-stretching phonon modes. In $CaSi_2$, which can be considered as the "antibonding analog" to MgB_2, the σ^* bands are strongly coupled to the bond-stretching phonons of the Si layer. In CaC_6 and CaAlSi, the so-called interlayer bands are filled and experience significant electron-phonon (*e*-ph) interaction to the out-of-plane buckling vibrations of the honeycomb layers.[7–11]

CaAlSi is of particular interest because it exhibits an ultrasoft phonon mode and crystallizes with several stacking variants.[12,13] The interplay of these two ingredients gives rise to intriguing effects on both normal and superconducting properties. The presence of an ultrasoft phonon mode at ~7 meV was initially evidenced by first-principles calculations[10,11,14–16] and recently confirmed by neutron-scattering experiments.[16] The ultrasoft phonon modes are believed to induce a strong *e*-ph coupling and to lead to an enhanced specific heat anomaly at T_c as well as to a *positive* pressure dependence of T_c in CaAlSi. These effects have not been observed in the isoelectronic and isostructural SrAlSi, which does not display any signature of soft phonon modes.[17]

Recent x-ray diffraction experiments on *nH*-CaAlSi single crystals revealed several stacking variations of two different types of Al-Si layers, denoted as *A* and *B* in the following (see Fig. 1). The *A* and *B* layers differ by a 60° rotation around the *c* axis.[12,13] Besides the simple 1*H* structure characterized by an $|A|A|A|\ldots$ stacking, two more stacking variants were found: 5*H* with an *AABBB* and 6*H* with an *AAABBB* sequence. Stacking of the *A* and *B* layers induces an internal stress on the structure, causing a buckling of *boundary layers*, i.e., layers with a different neighboring layer. Subsequent investigations show that the superconducting properties strongly depend on the kind of stacking of *A* and *B* layers.[13,18–20] However, all *ab initio* calculations, and analyses of the experimental data based thereon, so far have assumed that the stacking of Al-Si planes along the *c* axis is either uniform or completely disordered. To clarify the complex interplay of stacking variants, buckling, soft modes, and

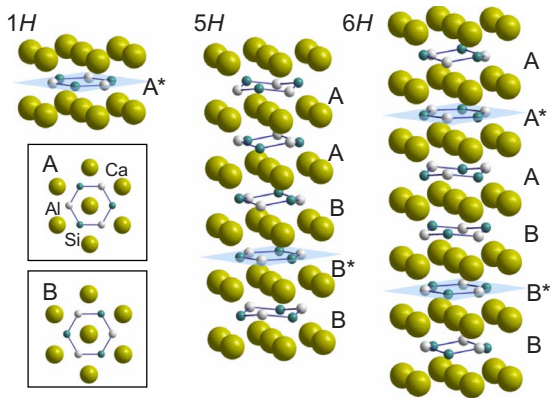

FIG. 1. (Color online) Crystal structure of 1*H*-, 5*H*-, and 6*H*-CaAlSi, which are characterized by a different sequence of *A* and *B* layers. *A* and *B* layers are rotated by 60° around the *c* axis with respect to each other. Flat and buckled Al-Si layers are indicated with and without an asterisk, respectively.

superconductivity, further investigation of the *e*-ph properties of different stacking variants of CaAlSi is highly desirable.

In this paper, we investigate the effects of pressure on the superconducting properties of *nH*-CaAlSi by experiments on single crystals and *ab initio* calculations of the *e*-ph properties. Previous experiments on polycrystalline samples of CaAlSi and SrAlSi showed that T_c of CaAlSi increases under pressure, while T_c of SrAlSi decreases.[17] In an *ab initio* study, Huang *et al.*[15] proposed that in 1*H*-CaAlSi, an enhancement of the *e*-ph coupling associated with the ultrasoft phonon modes can overcome the negative contribution of the other phonon branches and lead to an increase in T_c under pressure. Such an ultrasoft phonon mode was not obtained for SrAlSi.

However, recent experimental and theoretical results question these findings. First, until now, the pressure dependence of T_c in polycrystalline samples has been interpreted assuming a 1*H* stacking variant. However, here we will demonstrate that the pressure dependence of T_c for 1*H*-CaAlSi single crystals is markedly different from that of polycrystalline samples. Second, in these calculations,[15] the soft phonon branch in CaAlSi is unstable in some parts of the Brillouin zone, already at ambient pressure. This instability was not confirmed by recent *ab initio* calculations and neutron-scattering experiments.[11,16] Finally, Huang *et al.* assumed a uniform compressibility, which is very unlikely to occur in layered materials.

The aim of our analysis is twofold: on the one hand, we wish to investigate the interplay between soft modes and superconductivity in 1*H*-CaAlSi based on *ab initio* calculations and experiments on single crystals. On the other hand, we wish to understand how stacking variants affect the pressure dependence of the superconducting properties of CaAlSi.

Single crystals of CaAlSi were grown by using the floating zone method. Details of the crystal growth and characterization are described elsewhere.[13] The superconducting transition temperature (T_c) under pressure was determined by measuring the magnetic susceptibility in a superconducting quantum interference device magnetometer (Quantum Design). A Cu-Be piston-anvil-type pressure cell was used to apply quasihydrostatic pressures up to $P \sim 10$ kbars, with silicon oil or Fluorinert as a pressure transmitting medium. To monitor the pressure inside the pressure cell, we performed *in situ* measurements of the T_c of Sn (purity 99.999%) or Pb (purity 99.9999%).[21]

Figure 2 shows the temperature dependence of the magnetic susceptibility $[\chi(T)]$ of single crystals of *nH*-CaAlSi under pressures up to ~10 kbars. At ambient pressure, the T_cs of 1*H*-, 5*H*-, and 6*H*-CaAlSi are 6.50, 5.95, and 7.89 K, respectively, which are consistent with previous reports.[13] The superconducting transitions are relatively sharp for 1*H*- and 6*H*-CaAlSi with a transition width of $\Delta T_c \sim 0.1$ K at 80% of the diamagnetic shielding, indicating a good sample quality. For 5*H*-CaAlSi, the transition is broader ($\Delta T_c \sim 0.4$ K) but still sharp enough to follow its pressure dependence. With increasing pressure, the superconducting transition for 1*H*-CaAlSi clearly shifts to lower temperatures without a significant broadening of the transition. In contrast, the T_c in 5*H*- and 6*H*-CaAlSi increases with pressure. For all

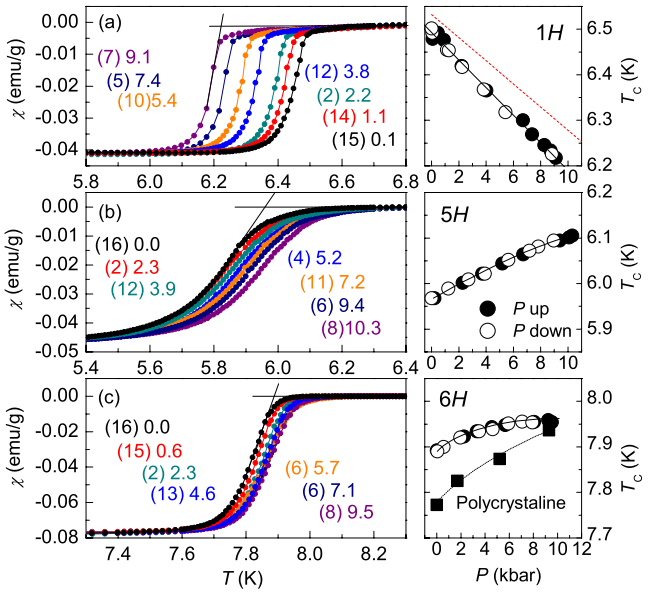

FIG. 2. (Color online) Left: Temperature dependence of the susceptibility for CaAlSi single crystals at different pressures. The numbers next to the data and in the parentheses correspond to the applied pressure (kbar) and the sequential order of the measurement runs, respectively. The extrapolation method to determine T_c is demonstrated with solid lines. Right: Pressure dependence of T_c for (a) 1*H*-, (b) 5*H*-, and (c) 6*H*-CaAlSi single crystals. For comparison, we plot the previous data for polycrystalline sample from Ref. 17 in (c) and the theoretical curve for $T_c(P)$ in (a) for 1*H*-CaAlSi with a (red) dashed line (Ref. 22).

samples, the T_c's and the shape of the $\chi(T)$ trace, taken after gradually releasing the pressure again, did agree with the data collected with increasing pressure.

Our measurements reveal that the pressure variation of T_c of *nH*-CaAlSi strongly depends on the stacking sequence. For a detailed comparison, T_c was identified as the temperature where the extrapolation of the steepest slope of $\chi(T)$ intersects the normal-state susceptibility extrapolated to lower temperatures. Using different criteria to determine T_c, e.g., the midpoint of the transition, changes the absolute value of T_c, but does not alter the relative variation of T_c. Surprisingly, for 1*H*-CaAlSi, T_c linearly decreases with a rate of $\Delta T_c/T_c = -0.03$ K/kbars, in contrast to a previous report on polycrystalline samples.[17] For 5*H*-CaAlSi, the pressure dependence is slightly nonlinear with an initial slope of +0.013 K/kbars, while 6*H*-CaAlSi exhibits a more pronounced nonlinear behavior and saturation at $T_c \sim 7.95$ K already at ~10 kbars.

In order to understand the effects of pressure and stacking variants on the superconducting properties of CaAlSi, we performed *ab initio* density-functional perturbation theory calculations[23–25] of the electronic and vibrational properties of *nH*-CaAlSi as a function of pressure. The computational details are given in Appendix B. Besides the identified 1*H*, 5*H*, and 6*H* stacking variants, we also considered hypothetical 2*H*- and 3*H*-CaAlSi, characterized by $|AB|AB|$ and $|AAB|AAB|$ stackings of the Al-Si planes, respectively.

In the investigated pressure range of up to 100 kbars, we

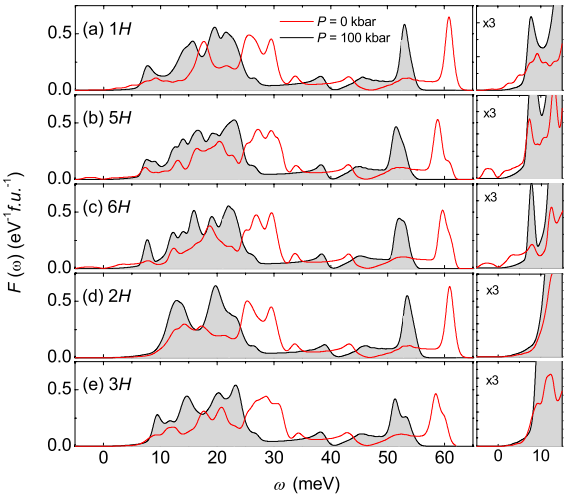

FIG. 3. (Color online) Linear response phDOS for different nH-CaAlSi at $P=0$ and $P=100$ kbars. In the right panel, we show an enlargement of the low-energy region.

relaxed the internal parameters of all structures at intervals of 20 kbars. The details of the optimization, together with the detailed band structures and phonon dispersion relations, will be published elsewhere. We subsequently fitted the E vs V curves to a Birch–Murnagham equation of state to obtain the equilibrium volume V_0 and the bulk modulus B_0 for each system. All equilibrium volumes and bulk moduli are close to each other ($68.6 \leq V_0 \leq 69.0$ Å^3, $49.6 \leq B_0 \leq 51.8$ GPa). In sign and magnitude, our calculations correctly reproduce the corrugation ("buckling") of the Al-Si planes in the $5H$ and $6H$ structures. A corrugation is also obtained for $3H$-CaAlSi. In contrast to previous suggestions,[12] the corrugation in the Al-Si layers of the $5H$ and $6H$ phases is not reduced by applying pressure. Rather, it remains unchanged for $6H$, or becomes even more pronounced for $5H$-CaAlSi. The compressibility is anisotropic, $k_c/k_a=3.8$, as expected for a layered material. At all pressures, the total energy of $2H$-CaAlSi and $3H$-CaAlSi is higher than that of $1H$-, $5H$-, and $6H$-CaAlSi, with the latter being almost degenerate in energy.[26]

By using the relaxed structures, we calculated by linear response the phonon frequencies $\omega_{\mathbf{q},\nu}$ and the e-ph linewidths, from which we obtained the Eliashberg spectral functions and the total electron-phonon coupling λ. In Fig. 3, we display the phonon density of states (phDOS) of nH-CaAlSi, calculated at the theoretical equilibrium pressure ($P=0$) and at the highest pressure considered (100 kbars). At $P=0$, the $1H$, $5H$, and $6H$ stacking variants all show a peak at ~ 7 meV, which is associated with the out-of-plane vibrations of the Al-Si planes. Under pressure, roughly one-half of the corresponding phonon states soften and drive the system to a structural instability at $P \sim 80$ kbars.[27] The corresponding phonon dispersions are shown in Appendix A. The hypothetical $2H$-CaAlSi and $3H$-CaAlSi, on the other hand, do not display the ultrasoft phonon peak at $P=0$, and all phonon modes harden with increasing pressure.

At present, we cannot conclusively explain the different phonon softening behavior of the systems. However, by comparing the (partial) phDOS's, which we obtained for different nH stacking variants with those of previous virtual crystal approximation calculations,[11,16] we observe that phonon softening mainly involves Al out-of-plane vibrations. Phonon softening appears if a block of three or more like planes are found in the sequence. This probably reflects the tendency of Al to form bonds with other Al atoms in the neighboring layers rather than sp^2 bonds with Si in the same layer, if the c lattice constant is small enough.

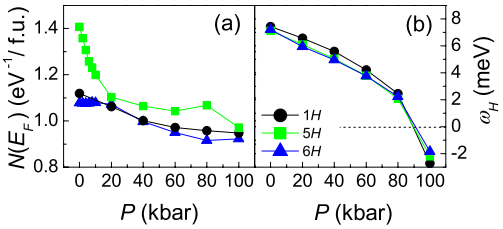

FIG. 4. (Color online) (a) Pressure dependence of the DOS at E_F and (b) frequency of the lowest-lying phonon branches at the H point for various nH-CaAlSi (Ref. 28).

Our results strongly differ from those of Ref. 15 for $1H$-CaAlSi. At $P=0$, our phonon frequencies are all real, and even at higher pressures, only a few become imaginary, while in Ref. 15, the whole out-of-plane branch becomes unstable. The most likely reason for this discrepancy is that we optimized the structural parameters, while the previous work assumed an isotropic compressibility. Also, a careful convergence of phonon frequencies with respect to $\mathbf{k}$ sampling and basis set size is crucial to obtain the correct behavior of the ultrasoft phonon modes.

If the coupling to the electrons is strong enough to overcome the opposing effect of the hardening of the other phonons and of the decrease in the electronic density of states (DOS) at the Fermi level, a soft phonon mode can lead to an increase in T_c with pressure. In Fig. 4, we show the calculated pressure dependences of the electronic DOS at the Fermi level, $N(E_F)$, and of the lowest lying phonon frequency at the H point (ω_H) for $1H$-, $5H$-, and $6H$-CaAlSi. We estimate the pressure evolution of the partial e-ph coupling constant associated with the soft phonon mode by using the Hopfield formula: $\lambda = N(E_F) I^2 / \omega_H^2$, where I is the e-ph matrix element. By assuming that I is independent of pressure, we estimate that the partial λ increases by $\sim 60\%$ for $1H$ and $6H$, and by $\sim 50\%$ for $5H$. For $2H$- and $3H$-CaAlSi (not shown), $N(E_F)$ decreases and ω_H increases, resulting in a net decrease in λ. From this argument, one could expect a very similar (increasing) behavior of T_c with pressure for $n=1$, 5, and 6. This is, however, not observed experimentally.

Figure 5 shows the evolution of the Eliashberg function $\alpha^2 F(\omega)$ of $1H$-CaAlSi for which we ran a full e-ph calculation as a function of pressure. In agreement with previous calculations,[11,16] at $P=0$ there is a large peak at $\omega \sim 7$ meV, which is associated with the Al-Si out-of-plane vibrations in the $k_z=\pi/c$ plane, implying that the corresponding phonon states have a considerable coupling to electrons. At higher pressures, following the behavior of the phDOS, this peak splits into two peaks, one of them softening,

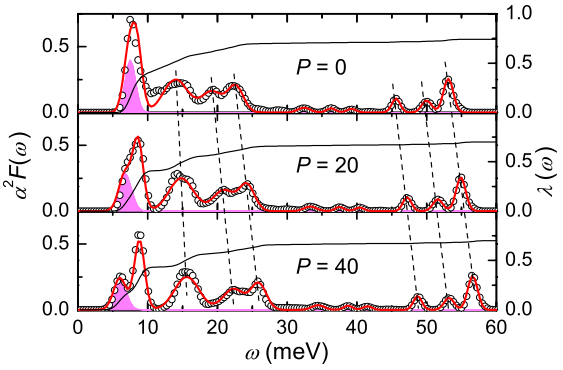

FIG. 5. (Color online) Evolution of the LDA Eliashberg function (open circles) $\alpha^2F(\omega)$ and $\lambda(\omega)$ with pressure (kbar) for 1*H*-CaAlSi. Red solid lines correspond to the simplified model with Gaussian peaks (described in the text). The resulting $\langle\omega_{ln}\rangle$ and λ are listed in Table I. The shaded area highlights the variation of energy and intensity for the ultrasoft phonon modes.

the other hardening with increasing pressure. The pressure-induced transfer of the spectral weight from the hard to the soft part of the low-lying peak affects both the total *e*-ph coupling parameter $\lambda=2\int_0^\infty \alpha^2F(\omega)\omega^{-1}d\omega$ and the logarithmic-averaged phonon frequency $\langle\omega_{\ln}\rangle$. By using the following Allen–Dynes equation:[30]

$$T_c=\frac{\langle\omega_{ln}\rangle}{1.2}\exp\left[\frac{-1.04(1+\lambda)}{\lambda-(1+0.62\lambda)\mu^*}\right], \quad (1)$$

where μ^* is the Coulomb pseudopotential, fixed to $\mu^*=0.1$ in the following (see Table I), we obtain a *decrease* in T_c with pressure for 1*H*-CaAlSi, which is in agreement with our experiments. A slight variation of μ^* does not alter this general behavior.

In stark contrast to the previous report for 1*H*-CaAlSi,[15] the effect of softening of the ultrasoft phonon modes is apparently not sufficient to overcome the opposing contributions from the other phonon branches. For further model calculations, we used a decomposition of $\alpha^2F(\omega)$ of 1*H*-CaAlSi into Gaussians, as shown in Fig. 5. Using this decomposition reveals that the behavior of T_c with pressure follows that of the spectral weight of the ultrasoft phonon mode, which decreases with pressure in 1*H*-CaAlSi. The change of the spectral weight of the ultrasoft phonon mode determines the behavior of T_c under pressure, more importantly than the decrease in its phonon frequency.

TABLE I. Calculated superconducting properties of 1*H*-CaAlSi as a function of pressure. T_c was obtained by the Allen–Dynes formula, with $\mu^*=0.1$. For comparison, we give the results for 2*H* in parentheses.

P (kbars)	$\langle\omega_{ln}\rangle$ (K)	λ	T_c (K)
0	139.2 (160)	0.73 (0.60)	5.35 (3.66)
20	139.9 (186)	0.70 (0.47)	4.86 (1.75)
40	134.0 (200)	0.70 (0.43)	4.65 (1.24)

For 5*H*- and 6*H*-CaAlSi, due to their very large unit cells (15 and 18 atoms, respectively) and the extreme sensitivity of the results to computational parameters, we did not perform a full *e*-ph calculation. Although there are some subtle differences in the electron and phonon dispersions, the results shown in Figs. 3 and 4 imply that the pressure dependence is qualitatively very close to that of 1*H*-CaAlSi [i.e., the $N(E_F)$'s and ω_H decrease with the same rate and a structural instability happens at elevated pressures]. For this reason, we assume that their $\alpha^2F(\omega)$'s have very similar characteristics to that of 1*H*-CaAlSi. The different pressure dependence of T_c for 5*H* and 6*H* therefore has to be attributed to a different (increasing) behavior of the spectral weight for the ultrasoft phonon mode under pressure. This behavior could reflect either small differences in *e*-ph matrix elements due to the buckling of some planes or a different number of phonon modes that soften under pressure.

Another aspect, which we cannot rule out completely, is that in 5*H*- or 6*H*-CaAlSi, multiband effects become relevant. Recently, Lupi *et al.*[20] reported an anisotropy of the optical response in the superconducting and normal states for a crystal with mixed 5*H* and 6*H* phases. The superconducting gap, determined by penetration depth measurements, also shows a sizable anisotropy, depending on the stacking sequences.[18] Further studies are needed to clarify this point. In particular, understanding the effect of buckling of the Al-Si layers on the anisotropy of the *e*-ph coupling appears to be the crucial issue.

We would like to emphasize once more that the hypothetical systems 2*H*- and 3*H*-CaAlSi show a completely different behavior. First, they are energetically disfavored with respect to existing stacking variants because of a nonoptimized energy balance between the formation of *AB* interfaces and buckling. Second, they do not display any soft phonon modes, which only appear if three or more Al atoms are arranged in a sequence along the *c* axis.

All phonon modes harden with pressure, leading to an increase in $\langle\omega_{ln}\rangle$, a fast decrease in λ, and a net decrease in T_c with pressure with a rate of $dT_c/dP\sim-0.05$ K/kbars. For comparison, the results for 2*H*-CaAlSi are also listed in Table I. Therefore, 2*H*- and 3*H*-CaAlSi do not represent proper models for other stacking variants.

In summary, we demonstrate that for single crystals of *n*H-CaAlSi, the behavior of T_c under pressure crucially depends on the particular stacking sequence and the buckling of the Al-Si layers. T_c *decreases* for 1*H* and *increases* with pressure in 5*H*- and 6*H*-CaAlSi. Previous experiments on polycrystalline samples gave results that are closer to the behavior of 6*H*-CaAlSi but adverse to the behavior of 1*H*-CaAlSi. One may speculate that the polycrystalline sample consisted mainly of phases with stacking variants other than 1*H*-CaAlSi. Based on our *ab initio* calculations, we find a gradual softening of an out-of-plane phonon mode under pressure for *n*H-CaAlSi ($n=1$, 5, and 6), which leads to a structural instability at higher pressures. In 1*H*-CaAlSi, the softening is not strong enough to lead to an increase in T_c, which is in contrast to previous calculations, while it is

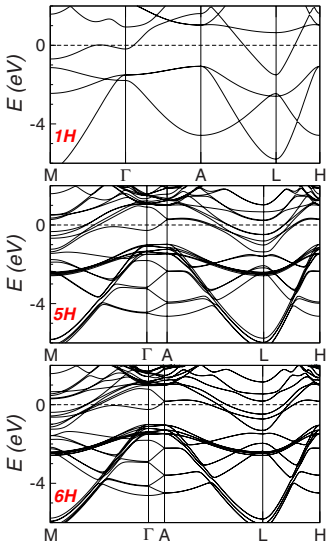

FIG. 6. (Color online) From top to bottom: Band structure of 1*H*-, 5*H*-, and 6*H*-CaAlSi at $P=0$.

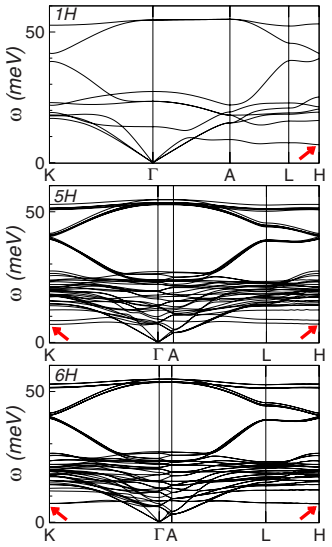

FIG. 7. (Color online) From top to bottom: Phonon dispersions of 1*H*-, 5*H*-, and 6*H*-CaAlSi at $P=0$.

likely that this softening leads to the increase in T_c with pressure in single crystals of 5*H*- and 6*H*-CaAlSi.

The authors acknowledge useful discussions with K. Syassen, A. Simon, O. K. Andersen, and G. B. Bachelet. We also thank E. Brücher and S. Höhn for experimental assistance.

APPENDIX A: ELECTRON AND PHONON DISPERSIONS

In this appendix, we briefly describe the main features of the electronic and phononic dispersion relations of 1*H*-, 5*H*-, and 6*H*-CaAlSi. A detailed discussion will be published elsewhere.[31]

Figure 6 shows the electronic structures at ambient pressure, which is in very good agreement with previous results.[11,29] The essential features are best discussed for 1*H*-CaAlSi. The band structures (and the Fermi surfaces) of 5*H*- and 6*H*-CaAlSi have features very similar to those of 1*H*-CaAlSi. The main difference is that, due to the additional *AB* interfaces and buckling of Al-Si layers, small gaps appear between the folded-in sheets of the interlayer hole Fermi surface along the Γ-*M* line.

At the Γ point, the top of the bonding σ bands is situated ~2 eV below E_F, crossed by the bonding π band. The band at ~0.2 eV below E_F has a significant Ca character, and it can be traced back to the interlayer band of graphite. It forms a small electron pocket in the Fermi surface around the Γ point and a larger hole pocket around the *M* point. The remaining tubular part of the Fermi surface, shown in Ref. 11, is due to the π^* band.

The phonon dispersion relations for the three stacking variants are shown in Fig. 7. In all cases, in-plane modes of the Al-Si layers are found at ~50 meV, and mixed Ca-Al-Si modes at ~20 meV. An ultrasoft optical mode with ω ~7 meV is found along the *A*-*L*-*H* line in 1*H*-CaAlSi. In 5*H*- and 6*H*-CaAlSi, due to zone folding, this single mode gives rise to an extremely flat branch along the *L*-*H*-*K*-*M* face of the Brillouin zone, marked by small arrows in the figure. An inspection of the eigenvector shows that this branch corresponds to an out-of-plane vibration of the Al-Si atoms. At the *H* point, this mode is almost purely Al like.

Figure 8 shows how electronic and phononic structures are modified by pressure. For simplicity, we only present results for 1*H*-CaAlSi. 5*H*- and 6*H*-CaAlSi show a very similar behavior. The left panel displays the evolution of the electronic structure with pressure. The electronic dispersion varies smoothly between $P=0$ and $P=100$ kbars, where the most significant difference is the disappearance of the small lenticular portion of the Fermi surface centered at the Γ point around $P=80$ kbars. Since this portion gives a minor contribution to the total DOS, the variation of the DOS with pressure is also rather smooth (see Fig. 4). The shape of the outer part of the Fermi surface is not affected by pressure.

On the other hand, the effect of pressure on the phonon dispersions is dramatic, as demonstrated in the right panel of Fig. 8. Here, we focus on the low-energy part of the spectrum ($\omega<20$ meV), which clearly shows that the optical branch at ~7 meV, indicated by small arrows in Fig. 7, considerably softens along the *A*-*L*-*H* line, until it finally

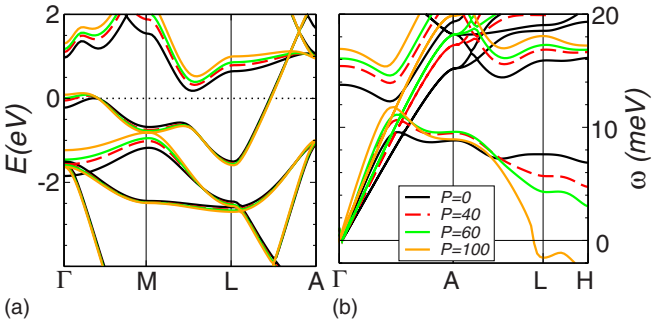

FIG. 8. (Color online) Evolution of the band structure of 1*H*-CaAlSi with pressure (kbar).

becomes unstable. The softening is continuous with pressure, which is in contrast to the results reported in Ref. 15. Other phonon branches (not shown) harden with pressure. 5*H*- and 6*H*-CaAlSi show a very similar behavior, with the modes marked by arrows softening under pressure and becoming unstable at $P \sim 80$ kbars.

APPENDIX B: COMPUTATIONAL DETAILS

The electronic, structural, and vibrational properties of all our crystals were calculated in the framework of the density-functional theory and of the density-functional perturbation theory,[23] with Kohn–Sham wave functions expanded on a plane-wave basis that is limited by a 40 Ryd cutoff energy.[24,25] We used Troullier–Martins[32] norm-conserving pseudopotentials generated by the FHI98PP package[33] and consistently employed the generalized gradient approximation Perdew–Burke–Emzerhof functional[34] to approximate the exchange-correlation energy functional. The **k**-space integration (electrons) was approximated with a $12\times12\times12$ Monkhorst–Pack grid[35] for the self-consistent cycles, with the more accurate tetrahedron method[36] and a $20\times20\times20$ mesh for the electronic DOS, and with an $18\times18\times18$ Monkhorst–Pack grid for the electron-phonon coupling. The smearing parameter[37] was set to 0.03 Ryd, which gave a convergence of the total energies within 0.1 mRyd, and 5 cm^{-1} for the phonon frequencies.

Dynamical matrices and electron-phonon linewidths $\gamma_{\mathbf{q},\nu}$ were evaluated on regular grids in **q** space (phonons). The phonon dispersions and the phDOS were then obtained by Fourier interpolation of the dynamical matrices, while the Eliashberg spectral functions $\alpha^2F(\omega)$ and the total *e*-ph coupling λs were calculated by summing over individual linewidths and frequencies.

In the present paper, we devoted special care to the convergence of the *e*-ph coupling functions with pressure, which turned out to critically depend on the **q**-space integration, particularly along the *c* direction. For the higher pressures, a $6\times6\times12$ **q** grid was found necessary to ensure convergence.

These **k** and **q** grids refer to the 1*H* case, and have been scaled according to the cell size for all other *n*. For 5*H*- and 6*H*-CaAlSi, as explained in the text, we did not perform a full electron-phonon coupling calculation, but we calculated the dynamical matrices on a 442 grid in **q** space and obtained the full dispersions by Fourier interpolation.

[1] J. Nagamatsu, N. Nakagawa, T. Muranaka, Y. Zenitani, and J. Akimitsu, Nature (London) **410**, 63 (2001).

[2] M. Imai, K. Nishida, T. Kimura, and H. Abe, Appl. Phys. Lett. **80**, 1019 (2002); M. Imai, El-Hadi S. Sadki, H. Abe, K. Nishida, T. Kimura, T. Sato, K. Hirata, and H. Kitazawa, Phys. Rev. B **68**, 064512 (2003).

[3] S. Sanfilippo, H. Elsinger, M. Núñez-Regueiro, O. Laborde, S. LeFloch, M. Affronte, G. L. Olcese, and A. Palenzona, Phys. Rev. B **61**, R3800 (2000); G. Satta, G. Profeta, F. Bernardini, A. Continenza, and S. Massidda, *ibid.* **64**, 104507 (2001).

[4] T. E. Weller, M. Ellerby, S. S. Saxena, R. P. Smith, and N. T. Skipper, Nat. Phys. **1**, 39 (2005).

[5] N. Emery, C. Hérold, M. d'Astuto, V. Garcia, Ch. Bellin, J. F. Marêché, P. Lagrange, and G. Loupias, Phys. Rev. Lett. **95**, 087003 (2005).

[6] J. S. Kim, L. Boeri, J. R. O'Brien, F. S. Razavi, and R. K. Kremer, Phys. Rev. Lett. **99**, 027001 (2007); J. S. Kim, L. Boeri, R. K. Kremer, and F. S. Razavi, *ibid.* **96**, 217002 (2006).

[7] M. Calandra and F. Mauri, Phys. Rev. Lett. **95**, 237002 (2005).

[8] L. Boeri, G. B. Bachelet, M. Giantomassi, and O. K. Andersen, Phys. Rev. B **76**, 064510 (2007).

[9] J. S. Kim, L. Boeri, R. K. Kremer, and F. S. Razavi, Phys. Rev. B **74**, 214513 (2006).

[10] I. I. Mazin and D. A. Papaconstantopoulos, Phys. Rev. B **69**, 180512(R) (2004).

[11] M. Giantomassi, L. Boeri, and G. B. Bachelet, Phys. Rev. B **72**, 224512 (2005).

[12] H. Sagayama, Y. Wakabayashi, H. Sawa, T. Kamiyama, A. Hoshikawa, S. Harjo, K. Uozato, A. K. Ghosh, M. Tokunaga, and T. Tamegai, J. Phys. Soc. Jpn. **75**, 043713 (2006).

[13] S. Kuroiwa, H. Sagayama, T. Kakiuchi, H. Sawa, Y. Noda, and J. Akimitsu, Phys. Rev. B **74**, 014517 (2006).

[14] G. Q. Huang, L. F. Chen, M. Liu, and D. Y. Xing, Phys. Rev. B **69**, 064509 (2004).

[15] G. Q. Huang, L. F. Chen, M. Liu, and D. Y. Xing, Phys. Rev. B **71**, 172506 (2005).

[16] R. Heid, K.-P. Bohnen, B. Renker, P. Adelmann, T. Wolf, D. Ernst, and H. Schober, J. Low Temp. Phys. **147**, 375 (2007).

[17] B. Lorenz, J. Cmaidalka, R. L. Meng, and C. W. Chu, Phys. Rev. B **68**, 014512 (2003).

[18] R. Prozorov, T. A. Olheiser, R. W. Giannetta, K. Uozato, and T. Tamegai, Phys. Rev. B **73**, 184523 (2006).

[19] S. Kuroiwa, T. Takasaki, T. Ekino, and J. Akimitsu, Phys. Rev. B **76**, 104508 (2007).

[20] S. Lupi, L. Baldassarre, M. Ortolani, C. Mirri, U. Schade, R. Sopracase, T. Tamegai, R. Fittipaldi, A. Vecchione, and P. Calvani, Phys. Rev. B **77**, 054510 (2008).

[21] A. Eiling and J. S. Schilling, J. Phys. F: Met. Phys. **11**, 623 (1981).

[22] In Fig. 2(a), to obtain the theoretical T_c, we used the Allen–Dynes formula with $\mu^*=0.072$ in order to match the experimental T_c at $P=0$. The other parameters are listed in Table I. In Fig. 2(c), the T_c vs P curve for polycrystalline samples is obtained from the raw susceptibility data of Ref. 17, using the same criteria for determining T_c that we used for single crystals.

[23] S. Baroni, S. Gironcoli, A. D. Corso, and P. Giannozzi, Rev. Mod. Phys. **73**, 515 (2001).

[24] http://www.pwscf.org

[25] X. Gonze, J.-M. Beuken, R. Caracas, F. Detraux, M. Fuchs, G.-M. Rignanese, L. Sindic, M. Verstraete, G. Zerah, F. Jollet, M. Torrent, A. Roy, M. Mikami, P. Ghosez, J. Y. Raty, and D. C. Allan, Comput. Mater. Sci. **25**, 478 (2002).

[26] Experimentally realized ($n=1$, 5, and 6) stacking variants are those for which the energy cost of creating *AB* interfaces is

compensated by the energy gain due to the buckling of *boundary layers*.

[27] Preliminary x-ray diffraction experiments confirm a structural instability for 1*H*-CaAlSi at ~9 GPa [J. S. Kim, X. Wang, K. Syassen, R. K. Kremer, and M. Hanfland (unpublished)].

[28] For consistency, we used the theoretical lattice constants at all pressures. At $P=0$, the deviation between the theoretical and experimental lattice constants is less than 1%, which has no effect on the calculated phonon frequencies for all systems and on the electronic DOS for 1*H* and 6*H*. For 5*H*, by using the experimental lattice constant at $P=0$, we obtain a much lower value for $N(E_F)=1.1$ st/eV f.u., which is in perfect agreement with other calculations (Ref. 29), and much closer to that of 1*H* and 6*H*.

[29] S. Kuroiwa, A. Nakashima, S. Miyahara, N. Furukawa, and J. Akimitsu, J. Phys. Soc. Jpn. **76**, 113705 (2007).

[30] P. B. Allen and R. C. Dynes, Phys. Rev. B **12**, 905 (1975).

[31] L. Boeri *et al.* (unpublished).

[32] N. Troullier and J. L. Martins, Phys. Rev. B **43**, 1993 (1991).

[33] M. Fuchs and M. Scheffler, Comput. Phys. Commun. **119**, 67 (1999).

[34] J. P. Perdew, K. Burke, and M. Ernzerhof, Phys. Rev. Lett. **77**, 3865 (1996).

[35] H. J. Monkhorst and J. D. Pack, Phys. Rev. B **13**, 5188 (1976).

[36] P. E. Blöchl, O. Jepsen, and O. K. Andersen, Phys. Rev. B **49**, 16223 (1994).

[37] N. Marzari, D. Vanderbilt, A. De Vita, and M. C. Payne, Phys. Rev. Lett. **82**, 3296 (1999).